Biochemical Pharmacology 81 (2011) 178–184

Contents lists available at ScienceDirect

Biochemical Pharmacology

journal homepage: www.elsevier.com/locate/biochempharm

LPS-induced dissociation of multidrug resistance-associated protein 2 (Mrp2) and radixin is associated with Mrp2 selective internalization in rats

Junjiro Saeki, Shuichi Sekine, Toshiharu Horie *

Laboratory of Biopharmaceutics, Graduate School of Pharmaceutical Sciences, Chiba University, Inohana 1-8-1, Chuo-ku, Chiba, 260-8675, Japan

ARTICLE INFO

Article history:
Received 14 June 2010
Accepted 16 September 2010

Keywords:
Biliary transporter
Radixin
Cholestasis
LPS
Internalization

ABSTRACT

Multidrug resistance-associated protein 2 (Mrp2) is an ATP-dependent export pump that mediates the formation of bile-salt-independent bile flow. Disruption of the canalicular localization of Mrp2, without changes in its expression, is observed in chronic liver failure and is accompanied by oxidative stress. We reported previously that Mrp2 is rapidly internalized from the canalicular membrane during acute oxidative stress induced by lipopolysaccharide (LPS) in the rat liver. A disturbance in the colocalization of Mrp2 and radixin (which crosslinks actin with interacting membrane proteins) and endocytic retrieval of Mrp2 are present in chronic liver failure. However, the C-terminal phosphorylation status of radixin (p-radixin; functional form) and its protein–protein interaction with Mrp2 were not examined in the pathological cholestatic situation. In this study, we examined whether the C-terminal phosphorylation status of radixin and its interaction with Mrp2 were affected by LPS-induced experimental liver failure with cholestasis, and whether this condition was accompanied by Mrp2 internalization in the rat liver. At 3 h after LPS treatment, the canalicular expression of Mrp2 was decreased, without variation of the other canalicular transporters. Similarly, the canalicular localization of radixin was decreased after LPS treatment. These results show that LPS treatment decreased the total amount of the active form of p-radixin and the amount of radixin that coimmunoprecipitated with Mrp2, and that LPS treatment impaired the protein–protein interaction between Mrp2 and radixin. In conclusion, LPS-induced cholestasis seems to be caused by posttranscriptional regulation of Mrp2, which is due to the disruption of its interaction with radixin and by its dephosphorylation.

1. Introduction

The multidrug resistance-associated protein 2 (MRP2) and the bile-salt export pump (BSEP/ABCB11) are involved in the formation of bile-salt-independent and -dependent bile flow, respectively. The canalicular secretion of several amphiphilic organic anions, including bilirubin glucuronides, glutathione (GSH), and its conjugates, is mediated by MRP2, which is a conjugate export pump encoded by the *mrp2* gene [1]. In addition to the static expression of MRP2 on the canalicular surface, its dynamic insertion and internalization processes are of great importance, as its steady-state expression level is directly dependent on these turnover rates. Therefore, disruption of these turnover rates is thought to lead to cholestatic jaundice. Oxidative stress markers are closely related with the progression of chronic cholestatic disorder in patients with chronic hepatic failure (primary biliary cirrhosis (PBC) and hepatitis C virus (HCV) infection) [2,3]. Disruption of the canalicular localization of MRP2, without variation in its expression, is observed in the liver of these patients [4]. Several studies demonstrated that experimental cholestasis induced by bile duct ligation (BDL) [5], taurolithocholic acid [6], estradiol-17β glucuronide [7], and phalloidin [8] is closely associated with impaired excretory function of Mrp2, which may be attributed to its endocytic retrieval from the canalicular membrane. We also demonstrated that Mrp2 internalization is observed under ethacrynic acid (EA)- and tert-butylhydroperoxide-induced acute oxidative stress in experimental perfused rat livers [9–11]. Moreover, oxidative-stress-triggered signaling pathways that lead to the activation of novel protein kinase C (nPKC) cause the rapid retrieval of Mrp2 from the canalicular surface in the rat liver [10]. In experimental liver failure with cholestasis,

Abbreviations: Mrp2, multidrug resistance-associated protein 2; Bsep, bile-salt export pump; PBC, primary biliary cirrhosis; HCV, hepatitis C virus; BDL, bile duct ligation; nPKC, novel protein kinase C; LPS, lipopolysaccharide; ERM, ezrin–radixin–moesin; F-actin, actin filament; cPKC, conventional PKC; Mdr1, multidrug resistance protein 1; DPPIV, dipeptidylpeptidase IV; ALT, alanine aminotransferase; CM, canalicular membrane; G-PBS, glycine-containing phosphate-buffered saline; ROS, reactive oxygen species; PDZ, postsynaptic density-95/Discs large/zona occludens-1; TLR4, toll-like receptor 4.

* Corresponding author. Tel.: +81 43 226 2886; fax: +81 43 226 2886.
E-mail address: horieto@p.chiba-u.ac.jp (T. Horie).

0006-2952/$ – see front matter © 2010 Elsevier Inc. All rights reserved.
doi:10.1016/j.bcp.2010.09.016

treatment with lipopolysaccharide (LPS), which is a bacterial endotoxin, causes the rapid retrieval of Mrp2 from the canalicular membrane [12]. In addition, we showed that oxidative stress is a triggering factor of LPS-induced Mrp2 internalization [13].

The ezrin–radixin–moesin (ERM) family of proteins crosslinks cytoskeletal actin filament (F-actin) with integral membrane proteins. This anchoring function of ERM is regulated by the C-terminal phosphorylation status of these proteins, via the transition between active (C-terminal phosphorylated) and inactive (C-terminal dephosphorylated) forms [14]. Radixin is the dominant ERM protein in the canalicular membrane of the liver. Mice lacking radixin develop conjugated hyperbilirubinemia because of the impaired localization of Mrp2 on the canalicular membrane surface, which suggests that radixin is required for the canalicular localization of Mrp2 [15]. Disturbed colocalization of Mrp2/MRP2 and radixin, as well as endocytic retrieval of MRP2, are observed in the liver of PBC patients and several experimental cholestatic models, which may be associated with a failure in the anchoring of Mrp2/MRP2 to the canalicular membrane [4,16–18]. However, the C-terminal phosphorylation status of radixin (p-radixin) and its protein–protein interaction with Mrp2/MRP2 were not examined in these pathological cholestatic situations. Recently, we demonstrated that the activation of conventional PKC (cPKC) impaired the localization of Mrp2 at the apical membrane surface of the rat intestine, but not of the multidrug resistance protein 1 (Mdr1, which is another apical membrane protein). This was accompanied by the downregulation of C-terminally phosphorylated ezrin (which is expressed dominantly in the intestine) and by a decrease in its interaction with Mrp2 [19]. Here, we propose that the LPS-induced alteration in the phosphorylation status of radixin may cause its dissociation from Mrp2 and lead to the internalization of Mrp2 in the rat liver. In addition, we examined whether the effect of LPS on protein localization was specific to Mrp2, rather than a nonspecific event accompanied by the internalization of other biliary transporters, such as Bsep and Mdr1.

2. Materials and methods

2.1. Chemicals and antibodies

LPS was obtained from Wako Pure Chemical (Osaka, Japan). A rabbit anti-Mrp2 polyclonal antibody (EAG15) was raised against the C-terminal 12-amino-acid sequence of rat Mrp2. Rabbit anti-phosphorylated ezrin (Thr567)/radixin (Thr564)/moesin (Thr558) (p-ERM) antibody was purchased from Millipore (Temecula, CA). Goat anti-rat/Alexa Fluor 488 and goat anti-mouse/Alexa Fluor 546 antibodies were from Molecular Probes (Eugene, OR). Mouse anti-Mrp2 (M_2III5) antibody was from Abcam (Cambridge, MA). Antiserum for rat Bsep (rBSEP) was raised in rabbits against an oligopeptide (the C-terminal sequence of rBSEP, AYYKLVITGAPIS) [20]. Anti-Mdr1 monoclonal antibody C219 was obtained from Zymed Laboratories, Inc. (San Francisco, CA). Rat anti-dipeptidyl-peptidase IV (DPPIV) antibody was obtained from BD Biosciences (San Jose, CA). Rat anti-radixin (R21) was generated by Dr Tsukita [21]. The horseradish-peroxidase-conjugated secondary antibodies used in the immunoblot analysis were from Santa Cruz Biotechnology, Inc. (Santa Cruz, CA). Anti β-actin antibody was obtained from Sigma–Aldrich (St. Louis, MO). All other chemicals and solvents were of analytical grade.

2.2. Animals

Male Wistar rats (130–160 g) were used throughout the experiments (SLC Japan Inc., Tokyo, Japan). All animals were treated humanely in accordance with the guidelines issued by the National Institutes of Health and all procedures described below were approved by the animal care committee of Chiba University.

2.3. Experimental design

Rats were injected with either LPS (4 mg/kg body weight) or vehicle (physiological saline, used as a control) via the tail vein. LPS from *Escherichia coli* O55 was dissolved in sterile physiological saline (0.9% NaCl, w/v). Animals were sacrificed 3 h after injection. To estimate oxidative stress and liver injury, the hepatic GSH content and leakage of alanine aminotransferase (ALT) into the serum were measured using conventional methods, as described previously [9,11].

2.4. Crude membrane preparation

The crude membrane (CrM) was prepared as described previously [22], with some modifications. For each sample, 2 g of frozen rat liver was thawed and cut up in 5 ml of cold 1 mM $NaHCO_3$, 0.5 mM PMSF, and protease inhibitor cocktail (5 μg/ml leupeptin and 1 μg/ml pepstatin A) and homogenized with a loose Dounce homogenizer (20 vertical strokes). The homogenate was diluted further in ice-cold 1 mM $NaHCO_3$/0.5 mM PMSF and centrifuged at $1500 \times g$ for 15 min at 4 °C. The pellet was resuspended in 5 ml 70% (w/w) sucrose. The homogenate was poured into a P40ST rotor tube (Hitachi, Japan) and overlaid with 4 ml of 44% and 4 ml of 36.5% (w/w) sucrose. The tube was centrifuged at $70{,}500 \times g$ for 90 min at 4 °C. The crude membrane fraction from the 36.5% to 44% interface was centrifuged in 1 mM $NaHCO_3$/0.5 mM PMSF at $58{,}800 \times g$ for 20 min at 4 °C. The pellet was resuspended in 500 μl 1 mM $NaHCO_3$, 0.5 mM PMSF, and protease inhibitors by repeated (10 times) suctioning through a 23-gauge needle. Alkaline phosphatase (ALP) activity (canalicular marker enzyme), Na^+/K^+ ATPase activity (plasma membrane marker enzyme) in the obtained membrane fraction were measured as previously described [22]. And, we used CrM which was highly concentrated more than 18–20 times (ALP activity) and 10–12 times (Na^+/K^+ ATPase activity) higher than that observed in each homogenate fraction. The sample was stored at −80 °C until further use.

2.5. Western blot analysis

The homogenate (60 μg of protein) and CrM (5 μg of protein for Mrp2 and DPPIV, 15 μg protein for Bsep and Mdr1, and 20 μg of protein for p-radixin) that were prepared from the rat liver were subjected to 8.5% polyacrylamide slab gel electrophoresis (containing 0.1% SDS) and transferred to an Immobilon-P Transfer Membrane filter (Millipore Corporation, Billerica, MA). The membrane was blocked overnight at 4 °C with TTBS (Tris-buffered saline with 0.05% Tween 20) containing 3% bovine serum albumin and probed at room temperature for 1 h using primary antibodies (EAG15 [1:1500], C219 [1:1500], rBSEP [1:1500], R21 [1:1500], anti-DPPIV [1:1500], p-ERM (p-radixin) [1:1000], and β-actin [1:1000]) diluted with TTBS containing 0.1% BSA. The membrane was incubated for 1 h at room temperature with secondary antibodies conjugated with horseradish peroxidase and diluted with TTBS containing 0.1% BSA. The membrane was detected by LAS 1000 (Fuji film, Tokyo, Japan) using enhanced chemiluminescence systems (GE Healthcare, Little Chalfont, Buckinghamshire, UK). The density of each band was normalized to the density of β-actin in the homogenate.

2.6. Immunoprecipitation analysis

Frozen livers were homogenized with 10 vertical strokes of a Teflon (DuPont, Wilmington, DE) homogenizer in lysis buffer

(1 ml/g of tissue (wet weight)) containing 25 mM Tris/HCl pH 7.5, 5 mM EDTA, 250 mM NaCl, 1% (v/v) Triton X-100, 60 mM n-octyl-β-D-glucopyranoside, 50 mM NaF, 1 mM Na_3VO_4, and protease inhibitors (1 mM PMSF, 5 μg/ml leupeptin, and 1 μg/ml pepstatin A) and were lysed in lysis buffer (25 μl/mg protein) for 1 h at 4 °C. The tissue homogenate (20 mg protein) and CrM (0.3 mg protein) obtained were centrifuged at 20,630 × *g* for 10 min and the resulting supernatant was collected as the tissue lysate and rotated overnight at 4 °C with protein G and the anti-Mrp2 antibody EAG15 (12 μl per 20 mg of protein of the tissue homogenate). The beads were sedimented at 9170 × *g* for 1 min and washed three times with wash buffer containing 25 mM Tris/HCl pH 7.5, 5 mM EDTA, 150 mM NaCl, 1% (v/v) Triton X-100, 50 mM NaF, and 1 mM Na_3VO_4. Finally, elution buffer containing 10 mM Tris/HCl pH 6.5, 3% (w/v) SDS, 10% (v/v) glycerol, 5% (v/v) β-mercaptoethanol, 8 M urea, and 0.001% bromophenol blue was added to the samples, which were boiled at 95 °C for 5 min. The suspension was centrifuged and the supernatant was subjected to SDS–polyacrylamide gel electrophoresis, followed by immunoblot analysis.

2.7. Immunofluorescence analysis

Small frozen liver blocks were embedded in Tissue-Tek O.C.T. Compound (Sakura Finetechnical Co. Ltd., Tokyo, Japan) and were used to prepare 5 μm-thick sections at −25 °C, which were then fixed in acetone at room temperature for 10 min. The sections on the slides were hydrated in 30 mM glycine-containing phosphate-buffered saline (G-PBS) for 15 min. Sections were then incubated with M_2III_5 (1:35) and R21 (1:35) antibodies for 1 h. After rinsing with G-PBS, the slides were incubated for 1 h with goat Alexa Fluor 546 anti-mouse IgG (1:150) and goat Alexa Fluor 488 anti-rat IgG (1:150). The antibodies were diluted in PBS containing 0.1% BSA. After rinsing with G-PBS, the slides were dipped in TBS for 5 min; subsequently, samples were mounted in VECTASHIELD (Vector Laboratories, Burlingame, CA). In some experiments, F-actin was stained with rhodamine–phalloidin (1:50 for 1 h; Invitrogen, Carlsbad, CA). After rinsing with G-PBS, the slides were dipped in TBS for 5 min; subsequently, the samples were mounted in VECTASHIELD. Immunofluorescence imaging was performed using a confocal laser-scanning microscope, LSM510 type (Carl Zeiss, Jena, Germany).

2.8. Statistical analysis

All data are presented as mean ± S.D. Statistical analysis were performed by ANOVA followed by the Bonferroni test. Differences were considered to be statistically significant if $P < 0.05$.

3. Results

3.1. Effect of LPS on the hepatic injury and redox statuses

LPS induces liver injury via the production of inflammatory cytokines and reactive oxygen species (ROS). We evaluated serum ALT level and hepatic GSH content as indexes of liver injury and oxidative stress, respectively. In LPS-treated rats, serum ALT leakage was significantly increased by about 10 times compared with the saline-treated control (Table 1). Hepatic GSH content was decreased by LPS treatment to 45.9 ± 8.2% of the saline-treated control (Table 1).

3.2. Effect of LPS on the localization of canalicular membrane proteins

Previous reports indicate that rapid retrieval of Mrp2 from the canalicular membrane is observed 3 h after LPS treatment [12]. However, other canalicular membrane proteins have not been examined. We examined whether other canalicular membrane proteins (i.e., Bsep, Mdr1, and DPPIV) were also internalized by the LPS injection. The expression of Mrp2 was decreased in the CrM (71.0 ± 5.5% of the saline-treated control), without changes in its expression in the rat liver homogenate (108.3 ± 26.3% of the saline-treated control; Fig. 1). In contrast, the expression of Bsep, Mdr1, and DPPIV was not changed by LPS treatment, either in the homogenate (104.6 ± 9.42%, 111.3 ± 17.5%, and 107.8 ± 18.1% of the control, respectively; Fig. 2) or in the CrM fraction (101.6 ± 20.8%, 106.1 ± 11.1%, and 107.2 ± 37.6% of the control, respectively; Fig. 2).

Table 1
Effect of LPS on hepatic injury and redox status.

	ALT (IU/L)	GSH (μmol/g liver)
Control	9.54 ± 1.20	1.70 ± 0.11
LPS	93.36 ± 48.60*	0.78 ± 0.15**

Rats were given LPS (4 mg/kg) or saline and were sacrificed at 3 h after the LPS treatment; subsequently serum and liver were collected and ALT leakage into serum and hepatic GSH content were measured. The results are given as the mean ± S.D. of three rats.
* $p < 0.05$.
** $p < 0.01$ compared with control.

3.3. Effect of LPS on the expression of radixin and p-radixin

The constitutive localization of Mrp2 is maintained by its interaction with proteins of the ERM family. We investigated the expression of total radixin (both activated and inactivated forms) and of C-terminally phosphorylated radixin (p-radixin) in the LPS-treated liver homogenate and CrM fraction. Total radixin expression, including the phosphorylated and dephosphorylated forms, in the homogenate was comparable to that observed in the saline-treated control (91.6 ± 9.6%; Fig. 3A), whereas the expression of total radixin in the CrM fraction was decreased by LPS treatment (41.5 ± 9.6% of the saline-treated control; Fig. 3A). In addition, the p-radixin content in the LPS-treated homogenate was also reduced compared with that observed for the saline-treated control (68.3 ± 6.8%; Fig. 3B). Moreover, the expression of p-radixin in the CrM fraction was more drastically decreased than that observed in the homogenate fraction after LPS treatment (26.6 ± 8.0% of the saline-treated control; Fig. 3B). These data suggest that C-terminally phosphorylated radixin is converted to its dephosphorylated form by LPS treatment.

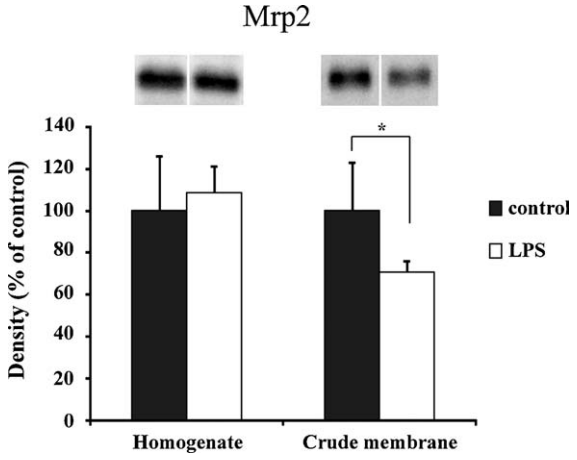

Fig. 1. . Effect of LPS treatment on the expression of Mrp2 in a liver homogenate and crude membrane (CrM) fraction. Rats were administered LPS (4 mg/kg body weight) or saline. The homogenate (60 μg of protein) and CrM fraction (5 μg of protein) were subjected to immunoblot analysis with anti-Mrp2 antibody (Mrp2 band density is shown below the blot). Band densities are expressed as a percentage of the saline-treated control value. Results are given as the mean ± S.D. of four independent rat livers. *$P < 0.05$ compared with the control.

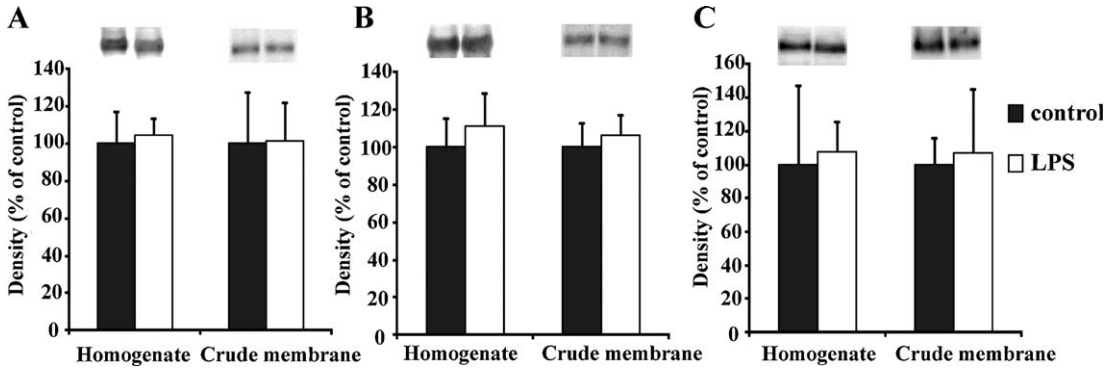

Fig. 2. . Effect of LPS treatment on the expression of canalicular membrane proteins (Bsep (A), Mdr1 (B), and DPPIV (C)). Rats were administered LPS (4 mg/kg body weight) or saline. The homogenate (60 μg of protein) and CrM fraction (5 μg or 15 μg of protein) were subjected to immunoblot analysis using antibodies for Bsep, Mdr1, and DPPIV (band densities of Bsep, Mdr1, and DPPIV are shown below the blot). Band densities are expressed as a percentage of the saline-treated control value. Results are given as the mean ± S.D. of four independent rat livers.

3.4. Effect of LPS on the protein–protein interaction of Mrp2 with radixin

To obtain insight into the molecular mechanism involved in the LPS-mediated downregulation of the surface expression of Mrp2, we investigated the molecular interaction of Mrp2 with radixin using immunoprecipitation analysis. In control tissues, radixin was readily coimmunoprecipitated with Mrp2, as described previously [15]. The interaction between Mrp2 and radixin was not detected when the preimmune rabbit IgG was used in the immunoprecipitation experiment (data not shown). The total expression of Mrp2 (Fig. 1) and the amount of Mrp2 immunoprecipitated with anti-Mrp2 antibody were not altered by LPS treatment, whereas the amount of radixin in the immunoprecipitate was decreased by LPS treatment in the homogenate (64.6 ± 9.6% of the saline-treated control; Fig. 4). In contrast, the amount of Mrp2 immunoprecipitated from the CrM fraction was reduced to 65.1 ± 8.3% of the control, to a similar extent as the decrease in Mrp2 content in the CrM fraction (Fig. 1) after LPS treatment. The extent of radixin downregulation (64.4 ± 32.0% of the control) in the coimmunoprecipitate from the CrM fraction was also comparable to the extent of LPS-induced downregulation of Mrp2 in the CrM fraction (Fig. 1) and of p-radixin downregulation in the homogenate fraction. These results suggest that the loss of Mrp2 from the canalicular membrane coincides with the loss of its interaction with radixin.

3.5. Effect of LPS on the colocalization of Mrp2 and radixin at the canalicular membrane

Mrp2 is physically supported by its interaction with proteins of the ERM family, as shown in hepatocytes and intestinal cells [15,23]. Several studies demonstrated a disturbance in the localization of Mrp2 and radixin in experimental cholestatic models [4,16–18]. We confirmed the dissociation of the protein–protein interaction of Mrp2 with radixin after LPS treatment (Fig. 4). Therefore, next we investigated the colocalization of Mrp2 and radixin using immunofluorescence analysis. In the control liver tissue, colocalization of Mrp2 and radixin was observed at the canalicular membrane. In contrast, LPS treatment led to the disruption of the canalicular localization of Mrp2 and radixin and to the partial disruption of the colocalization of Mrp2 and radixin in the cytoplasmic compartment, as indicated by the arrows in Fig. 5.

3.6. Effect of LPS on the integrity of F-actin in the pericanalicular domain

Disorganization of F-actin is observed in oxidative stress-induced cholestasis [24]. In addition, phalloidin, which is an inhibitor of F-actin depolymerization, induces internalization of Mrp2 and Mdr1 because of the overall disruption of the organization of pericanalicular F-actin [8]. In this study, we

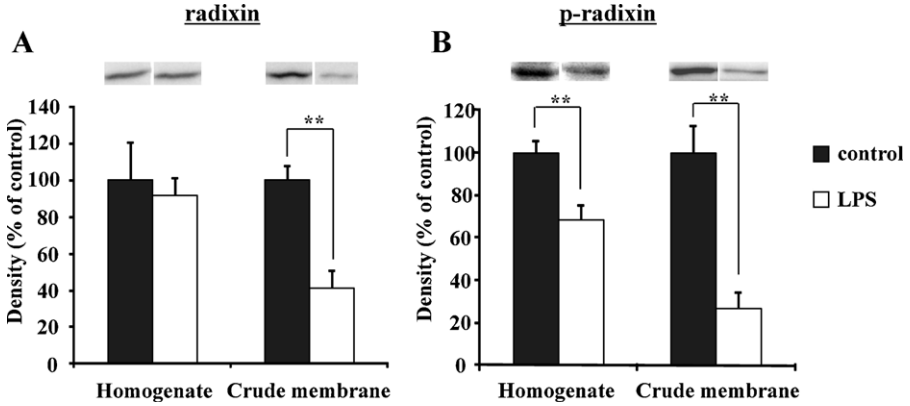

Fig. 3. . Effect of LPS treatment on the localization of total radixin (both activated and inactivated forms) and on the expression of C-terminally phosphorylated radixin (p-radixin). Rats were administered LPS (4 mg/kg body weight) or saline. The homogenate (60 μg of protein) and crude membrane fraction (5 μg or 20 μg of protein) were subjected to immunoblot analysis using radixin and p-radixin antibodies (band densities of radixin (A) and p-radixin (B) are shown below the blot). Band densities are expressed as a percentage of the saline-treated control value. Results are given as the mean ± S.D. of four independent rat livers. $^{*}P < 0.05$ compared with the control.

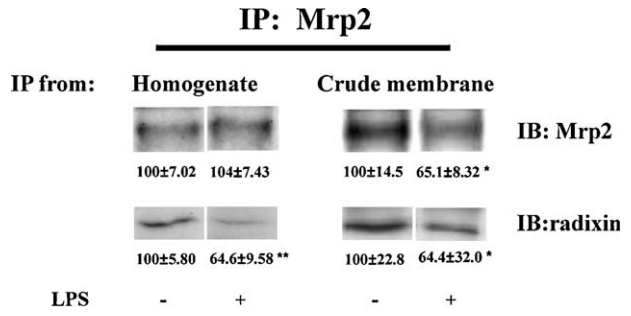

Fig. 4. . Effect of LPS treatment on the protein–protein interaction between Mrp2 and radixin. The lysates or CrM of treated rat livers were subjected to immunoprecipitation (IP) using the anti-Mrp2 antibody. Immunoprecipitates from lysates (left) or CrM (right) were subjected to immunoblot (IB) analysis using anti-Mrp2 and radixin antibodies (band densities of immunoprecipitated Mrp2 and radixin are shown below the blot). The values are expressed as a percentage of the saline-treated control value. Results are given as the mean ± S.D. of three (IP from homogenate) or four (IP from CrM) independent rat livers. $^{*}P < 0.05$ and $^{**}P < 0.01$ compared with the control.

confirmed the effect of LPS on the integrity of F-actin in the pericanalicular membrane. As a result, the integrity and localization of pericanalicular F-actin were not affected in the LPS-treated liver tissue (Fig. 6).

4. Discussion

Impaired steady-state canalicular surface expression of Mrp2 and jaundice are observed in radixin knockout mice. Therefore, radixin is now considered as the primary molecule that anchors Mrp2 to F-actin [15]. In parallel with this study, we revealed that the LPS-induced rapid retrieval of Mrp2 from the canalicular surface accompanied by GSH decrease is also triggered by oxidative stress [13]. In the present study, Mrp2 expression at the canalicular membrane was reduced to 71%, without changing the total expression of Mrp2, and canalicular Mrp2 localization was diffused into the cytosolic compartment, as assessed using immunofluorescence analysis (Figs. 1 and 5). More interestingly,

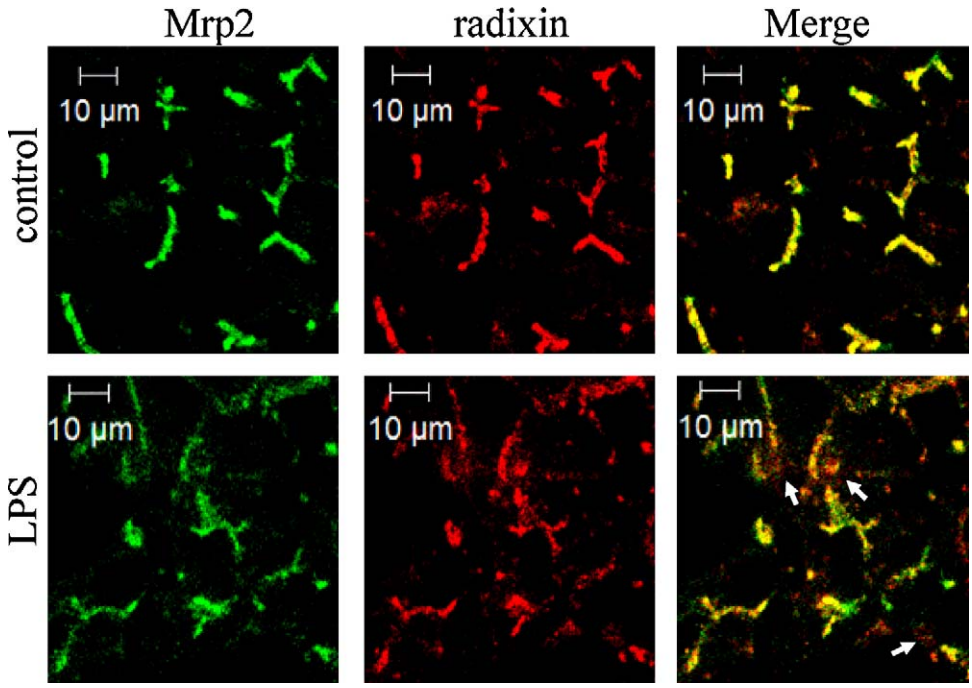

Fig. 5. Effect of LPS treatment on the distribution of Mrp2 and radixin in the rat liver. Immunofluorescence analysis (confocal laser-scanning microscopy) of the rat liver. Frozen sections (5 μm in thickness) of acetone-fixed tissue were stained with anti-Mrp2 (green) and -radixin (red) antibodies and examined using a confocal laser-scanning microscope. Disrupted colocalization of Mrp2 and radixin in the cytoplasmic compartment is represented by the arrows. Scale bar, 10 μm. (For interpretation of the references to color in this figure legend, the reader is referred to the web version of this article.)

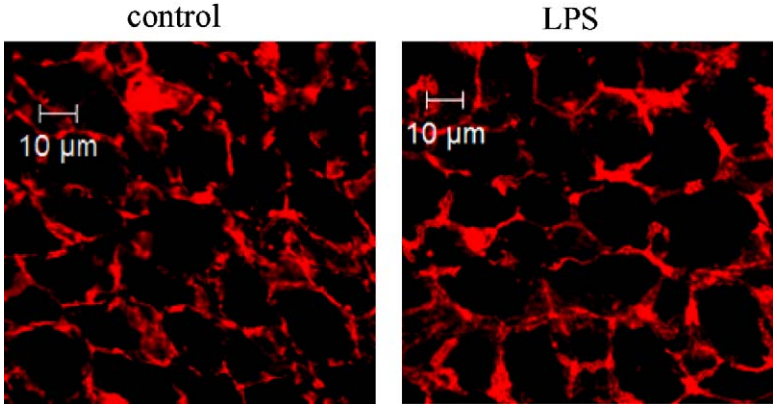

Fig. 6. Effect of LPS on the integrity of F-actin in the pericanalicular domain in the rat liver. Frozen sections (5 μm in thickness) of acetone-fixed tissue were stained with rhodamine–phalloidin and examined using a confocal laser-scanning microscope. Scale bar, 10 μm.

other apical membrane proteins, including Bsep, Mdr1, and DPPIV, were not altered after LPS treatment, in terms of their localization at the canalicular membrane (Fig. 2). Disruption of the pericanalicular actin cytoskeleton structure appears to be one of the common features of cholestasis. Phalloidin induces internalization of Mrp2 and Mdr1 because of the overall disorganization of pericanalicular F-actin [8]. We have previously indicated that this selective internalization was likely attributable to isoform-specific activation of PKC, without an effect on the structure of the actin cytoskeleton [10,11]. In this study, we confirmed that the effect of LPS on the localization of the biliary transporter was selective for Mrp2 and that the organization of F-actin was not disrupted by the LPS treatment. In contrast, it was reported that canalicular Bsep localization in the rat liver is also affected after a 6 h LPS treatment [22]. We have previously reported that nPKCs, including PKCδ and PKCε, are selectively activated by EA-induced oxidative stress and Mrp2-specific internalization in rat hepatocyte [10]. On the other hand, the cPKC activator thymeleatoxin induced Bsep internalization in a rat liver perfusion model [25]. Thus, two canalicular biliary transporters (Mrp2 and Bsep) are distinctly internalized in a PKC subfamily-dependent manner. The distinct behavior of these two canalicular transporters is well known, especially as tauroursodeoxycholate and genipin recruit Bsep and Mrp2 specifically to the canalicular membrane surface, respectively [26,27]. Based on this consideration, it is not surprising that LPS-induced oxidative stress leads to the selective internalization of Mrp2 under this experimental condition. It is possible that the signaling that regulates the translocation of these transporters consists of multiple pathways that overlap partially or cross each other [28]. These findings suggest that LPS-induced Mrp2 internalization was not caused solely by a disruption of canalicular structures. Rather, it should be noted that a series of signaling pathways that lead to the selective activation of nPKC are thought to be involved in this mechanism, as we have previously demonstrated in an EA-induced acute oxidative stress model; however, it remains unclear whether the cPKC-dependent internalization of Bsep internalization occurred in the 6 h that followed LPS treatment.

In line with this study, we have also reported that cPKC activation by thymeleatoxin alters the C-terminal phosphorylation status of ezrin and its interaction with Mrp2, which causes Mrp2 internalization in the rat intestine [19]. In the liver, Mrp2 retention in the canalicular membrane requires the interaction between radixin and the postsynaptic density-95/Discs large/zona occludens-1 (PDZ)-binding motif located in the C terminus of Mrp2 [29,30]. Mrp2 is thought to be stably expressed in the apical membrane by binding to radixin directly through the PDZ-binding motif or indirectly mediated by PDZ proteins (i.e., Na^+–H^+ exchanger regulatory factor 1 and PDZ domain-containing 1). Although, previous reports indicated that Mdr1 could interact with ezrin in rat intestine [19], and also interact with each ERM proteins in human T-lymphocytes [31]. Bsep and Mdr1 do not have obvious PDZ-interacting motifs in their C terminals and the localization of Mdr1 and DPPIV at the apical membrane surface is not affected in the liver of radixin knockout mice [15]. In addition, we did not confirm the interaction between Mdr1 and radixin in the rat liver, as was reported previously for the radixin knockout mouse [15] (Supplemental Fig. 1). The interaction of Mdr1 with proteins of the ERM family may depend on the subfamily or the organs. These observations lead us to postulate that the LPS-induced selective internalization of Mrp2 is due to changes in the protein–protein interaction of radixin with the PDZ-binding motif located in the C terminus of Mrp2; however, it remains unclear whether the protein–protein interaction of Mrp2 with radixin involves the direct binding of the proteins.

The disruption of the colocalization of Mrp2 with radixin was reported in several cholestatic liver diseases and in animal models of cholestasis, such as BDL and ethinyl estradiol-treated rats [17,18]. However, there is no report evaluating the C-terminal phosphorylation status of radixin and its interaction with Mrp2 in a cholestatic model that exhibits Mrp2 internalization. Mrp2 internalization accompanied by disruption of the colocalization of Mrp2 with radixin was also observed after LPS treatment. Our results suggest that LPS induces the dephosphorylation of radixin and the disruption of the binding between Mrp2 and radixin, which decrease the stability of the expression of Mrp2 at the apical membrane, leading to the internalization of Mrp2 in the rat liver. Dephosphorylated radixin adopts an inactive conformation via intramolecular/intermolecular interactions between its N-terminal and C-terminal domains. The inactive form of radixin loses its ability to bind membrane proteins and the cytoskeleton because its N and C termini are masked. It was reported that C-terminally dephosphorylated mutant ezrin (T567A) is distributed diffusely in the cytoplasm, whereas phosphorylated mutant ezrin (T567D) is distinctly localized at the membrane surface, which indicates that the membrane localization of radixin is strictly dependent on its C-terminal phosphorylation status [32]. Our data also suggests that the LPS-induced dephosphorylation form of radixin is not retained near the cell surface and is transferred to the intracellular space, as shown in Figs. 3 and 5. Concomitantly, Mrp2 and radixin did not colocalize in the cytosolic compartment because the inactive conformation of dephosphorylated radixin did not interact with internalized Mrp2, which suggests that these proteins were relocated from the canalicular membrane to the cytosolic compartment via distinct pathways, after disruption of their interaction (see graphical abstract).

Multiple kinases [33–35] and putative protein phosphatases [36] are involved in the phosphorylation and dephosphorylation of the C-terminal threonine residue of ERM proteins, to regulate the balance between their active and inactive forms. We described previously the involvement of PKC in Mrp2 internalization under oxidative stress conditions. The results of the present study suggest that alteration of the radixin phosphorylation status also correlated with PKC activation, as seen in the cPKC-dependent dephosphorylation of ezrin in the rat intestine [19]. In our preliminary study, the combined use of a PKC inhibitor suppressed LPS-induced ALT leakage and decreased intracellular GSH content (data not shown). These observations indicate that the combined use of a PKC inhibitor is not suitable for the investigation of the putative role of PKC in the LPS-induced dephosphorylation of radixin.

In conclusion, LPS-induced cholestasis is caused by posttranscriptional regulation of Mrp2, which is associated with the disruption of its interaction with radixin and by its dephosphorylation.

Acknowledgments

We thank Prof. Sachiko Tsukita for kindly providing the rat anti-radixin (R21) antibody. This work was supported by a Grant-in-Aid for Scientific Research (A) (21249003) and a Grant-in-Aid for Young Scientists (B) (21790141) from the Ministry of Education, Culture, Sports, Science and Technology of Japan.

Appendix A. Supplementary data

Supplementary data associated with this article can be found, in the online version, at doi:10.1016/j.bcp.2010.09.016.

References

[1] Jedlitschky G, Leier I, Buchholz U, Hummel-Eisenbeiss J, Burchell B, Keppler D. ATP-dependent transport of bilirubin glucuronides by the multidrug resistance protein MRP1 and its hepatocyte canalicular isoform MRP2. Biochem J 1997;327(Pt 1):305–10.

[2] Aboutwerat A, Pemberton PW, Smith A, Burrows PC, McMahon RF, Jain SK, et al. Oxidant stress is a significant feature of primary biliary cirrhosis. Biochim Biophys Acta 2003;1637(2):142–50.
[3] Maki A, Kono H, Gupta M, Asakawa M, Suzuki T, Matsuda M, et al. Predictive power of biomarkers of oxidative stress and inflammation in patients with hepatitis C virus-associated hepatocellular carcinoma. Ann Surg Oncol 2007;14(3):1182–90.
[4] Kojima H, Nies AT, Konig J, Hagmann W, Spring H, Uemura M, et al. Changes in the expression and localization of hepatocellular transporters and radixin in primary biliary cirrhosis. J Hepatol 2003;39(5):693–702.
[5] Paulusma CC, Kothe MJ, Bakker CT, Bosma PJ, van Bokhoven I, van Marle J, et al. Zonal down-regulation and redistribution of the multidrug resistance protein 2 during bile duct ligation in rat liver. Hepatology 2000;31(3):684–93.
[6] Beuers U, Bilzer M, Chittattu A, Kullak-Ublick GA, Keppler D, Paumgartner G, et al. Tauroursodeoxycholic acid inserts the apical conjugate export pump, Mrp2, into canalicular membranes and stimulates organic anion secretion by protein kinase C-dependent mechanisms in cholestatic rat liver. Hepatology 2001;33(5):1206–16.
[7] Mottino AD, Cao J, Veggi LM, Crocenzi F, Roma MG, Vore M. Altered localization and activity of canalicular Mrp2 in estradiol-17beta-D-glucuronide-induced cholestasis. Hepatology 2002;35(6):1409–19.
[8] Rost D, Kartenbeck J, Keppler D. Changes in the localization of the rat canalicular conjugate export pump Mrp2 in phalloidin-induced cholestasis. Hepatology 1999;29(3):814–21.
[9] Ji B, Ito K, Sekine S, Tajima A, Horie T. Ethacrynic-acid-induced glutathione depletion and oxidative stress in normal and Mrp2-deficient rat liver. Free Radic Biol Med 2004;37(11):1718–29.
[10] Sekine S, Ito K, Horie T. Oxidative stress and Mrp2 internalization. Free Radic Biol Med 2006;40(12):2166–74.
[11] Sekine S, Ito K, Horie T. Canalicular Mrp2 localization is reversibly regulated by the intracellular redox status. Am J Physiol Gastrointest Liver Physiol 2008;295(5):G1035–41.
[12] Kubitz R, Wettstein M, Warskulat U, Haussinger D. Regulation of the multidrug resistance protein 2 in the rat liver by lipopolysaccharide and dexamethasone. Gastroenterology 1999;116(2):401–10.
[13] Yano K, Sekine S, Nemoto K, Fuwa T, Horie T. The effect of dimerumic acid on LPS-induced downregulation of Mrp2 in the rat. Biochem Pharmacol 2010;80(4):533–9.
[14] Ishikawa H, Tamura A, Matsui T, Sasaki H, Hakoshima T, Tsukita S, et al. Structural conversion between open and closed forms of radixin: low-angle shadowing electron microscopy. J Mol Biol 2001;310(5):973–8.
[15] Kikuchi S, Hata M, Fukumoto K, Yamane Y, Matsui T, Tamura A, et al. Radixin deficiency causes conjugated hyperbilirubinemia with loss of Mrp2 from bile canalicular membranes. Nat Genet 2002;31(3):320–5.
[16] Kojima H, Sakurai S, Uemura M, Kitamura K, Kanno H, Nakai Y, et al. Disturbed colocalization of multidrug resistance protein 2 and radixin in human cholestatic liver diseases. J Gastroenterol Hepatol 2008;23(7 Pt 2):e120–8.
[17] Kojima H, Sakurai S, Yoshiji H, Uemura M, Yoshikawa M, Fukui H. The role of radixin in altered localization of canalicular conjugate export pump Mrp2 in cholestatic rat liver. Hepatol Res 2008;38(2):202–10.
[18] Rost D, Kloeters-Plachky P, Stiehl A. Retrieval of the rat canalicular conjugate export pump Mrp2 is associated with a rearrangement of actin filaments and radixin in bile salt-induced cholestasis. Eur J Med Res 2008;13(7):314–8.
[19] Nakano T, Sekine S, Ito K, Horie T. Correlation between apical localization of Abcc2/Mrp2 and phosphorylation status of ezrin in rat intestine. Drug Metab Dispos 2009;37(7):1521–7.
[20] Akita H, Suzuki H, Ito K, Kinoshita S, Sato N, Takikawa H, et al. Characterization of bile acid transport mediated by multidrug resistance associated protein 2 and bile salt export pump. Biochim Biophys Acta 2001;1511(1):7–16.
[21] Doi Y, Itoh M, Yonemura S, Ishihara S, Takano H, Noda T, et al. Normal development of mice and unimpaired cell adhesion/cell motility/actin-based cytoskeleton without compensatory up-regulation of ezrin or radixin in moesin gene knockout. J Biol Chem 1999;274(4):2315–21.
[22] Vos TA, Hooiveld GJ, Koning H, Childs S, Meijer DK, Moshage H, et al. Up-regulation of the multidrug resistance genes, Mrp1 and Mdr1b, and down-regulation of the organic anion transporter, Mrp2, and the bile salt transporter, Spgp, in endotoxemic rat liver. Hepatology 1998;28(6):1637–44.
[23] Yang Q, Onuki R, Nakai C, Sugiyama Y. Ezrin and radixin both regulate the apical membrane localization of ABCC2 (MRP2) in human intestinal epithelial Caco-2 cells. Exp Cell Res 2007;313(16):3517–25.
[24] Roma MG, Milkiewicz P, Elias E, Coleman R. Control by signaling modulators of the sorting of canalicular transporters in rat hepatocyte couplets: role of the cytoskeleton. Hepatology 2000;32(6):1342–56.
[25] Kubitz R, Saha N, Kuhlkamp T, Dutta S, vom Dahl S, Wettstein M, et al. Ca^{2+}-dependent protein kinase C isoforms induce cholestasis in rat liver. J Biol Chem 2004;279(11):10323–30.
[26] Kubitz R, Sutfels G, Kuhlkamp T, Kolling R, Haussinger D. Trafficking of the bile salt export pump from the Golgi to the canalicular membrane is regulated by the p38 MAP kinase. Gastroenterology 2004;126(2):541–53.
[27] Shoda J, Miura T, Utsunomiya H, Oda K, Yamamoto M, Kano M, et al. Genipin enhances Mrp2 (Abcc2)-mediated bile formation and organic anion transport in rat liver. Hepatology 2004;39(1):167–78.
[28] Crocenzi FA, Mottino AD, Roma MG. Regulation of synthesis and trafficking of canalicular transporters and its alteration in acquired hepatocellular cholestasis. Experimental therapeutic strategies for its prevention. Curr Med Chem 2004;11(4):501–24.
[29] Harris MJ, Kuwano M, Webb M, Board PG. Identification of the apical membrane-targeting signal of the multidrug resistance-associated protein 2 (MRP2/MOAT). J Biol Chem 2001;276(24):20876–81.
[30] Kocher O, Comella N, Gilchrist A, Pal R, Tognazzi K, Brown LF, et al. PDZK1, a novel PDZ domain-containing protein up-regulated in carcinomas and mapped to chromosome 1q21, interacts with cMOAT (MRP2), the multidrug resistance-associated protein. Lab Invest 1999;79(9):1161–70.
[31] Luciani F, Molinari A, Lozupone F, Calcabrini A, Lugini L, Stringaro A, et al. P-glycoprotein-actin association through ERM family proteins: a role in P-glycoprotein function in human cells of lymphoid origin. Blood 2002;99(2):641–8.
[32] Lee JH, Katakai T, Hara T, Gonda H, Sugai M, Shimizu A. Roles of p-ERM and Rho-ROCK signaling in lymphocyte polarity and uropod formation. J Cell Biol 2004;167(2):327–37.
[33] Belkina NV, Liu Y, Hao JJ, Karasuyama H, Shaw S. LOK is a major ERM kinase in resting lymphocytes and regulates cytoskeletal rearrangement through ERM phosphorylation. Proc Natl Acad Sci U S A 2009;106(12):4707–12.
[34] Hebert M, Potin S, Sebbagh M, Bertoglio J, Breard J, Hamelin J. Rho-ROCK-dependent ezrin–radixin–moesin phosphorylation regulates Fas-mediated apoptosis in Jurkat cells. J Immunol 2008;181(9):5963–73.
[35] Jeon S, Kim NH, Kim JY, Lee AY. Stem cell factor induces ERM proteins phosphorylation through PI3K activation to mediate melanocyte proliferation and migration. Pigment Cell Melanoma Res 2009;22(1):77–85.
[36] Zhu L, Zhou R, Mettler S, Wu T, Abbas A, Delaney J, et al. High turnover of ezrin T567 phosphorylation: conformation, activity, and cellular function. Am J Physiol Cell Physiol 2007;293(3):C874–84.